

Research Paper

3,3'-Diindolylmethane stimulates exosomal Wnt11 autocrine signaling in human umbilical cord mesenchymal stem cells to enhance wound healing

Hui Shi^{1*}, Xiao Xu^{1*}, Bin Zhang^{1*}, Jiahao Xu¹, Zhaoji Pan¹, Aihua Gong¹, Xu Zhang¹, Rong Li¹, Yaoxiang Sun¹, Yongmin Yan¹, Fei Mao¹, Hui Qian¹, Wenrong Xu^{1*}

1. Jiangsu Key Laboratory of Medical Science and Laboratory Medicine, School of Medicine, Jiangsu University, Zhenjiang, Jiangsu 212013, China;
2. The Affiliated Hospital, Jiangsu University, Zhenjiang, Jiangsu 212013, China.

* These authors have contributed equally to this work.

 Corresponding authors: Wenrong Xu, PhD, MD, Professor, School of Medicine, Jiangsu University, 301 Xuefu Road, Jiangsu 212013, China Tel: +86 511 85038215 Fax: +86 511 85038483 E-mail: icls@ujs.edu.cn; Hui Qian, PhD, Professor, School of Medicine, Jiangsu University, 301 Xuefu Road, Jiangsu 212013, China Tel: +86 511 85038334 Fax: +8651185038483 E-mail: lstormmlst@163.com

© Ivyspring International Publisher. This is an open access article distributed under the terms of the Creative Commons Attribution (CC BY-NC) license (<https://creativecommons.org/licenses/by-nc/4.0/>). See <http://ivyspring.com/terms> for full terms and conditions.

Received: 2016.10.26; Accepted: 2017.02.23; Published: 2017.04.10

Abstract

Human umbilical cord-derived mesenchymal stem cells (hucMSCs) are suggested as a promising therapeutic tool in regenerative medicine, however, their efficacy requires improvement. Small molecules and drugs come up to be a convenient strategy in regulating stem cells fate and function. Here, we evaluated 3,3'-diindolylmethane (DIM), a natural small-molecule compound involved in the repairing effects of hucMSCs on a deep second-degree burn injury rat model. HucMSCs primed with 50 μ M of DIM exhibited desirable repairing effects compared with untreated hucMSCs. DIM enhanced the stemness of hucMSCs, which was related to the activation of Wnt/ β -catenin signaling. β -catenin inhibition impaired the healing effects of DIM-primed hucMSCs (DIM-hucMSCs) *in vivo*. Moreover, we demonstrated that DIM upregulated Wnt11 expression in hucMSC-derived exosomes. Wnt11 knockdown inhibited β -catenin activation and stemness induction in DIM-hucMSCs and abrogated their therapeutic effects *in vivo*. Thus, our findings indicate that DIM promotes the stemness of hucMSCs through increased exosomal Wnt11 autocrine signaling, which provides a novel strategy for improving the therapeutic effects of hucMSCs on wound healing.

Key words: 3,3'-diindolylmethane; wound healing; Wnt11; exosome.

Introduction

The skin is the largest barrier in the human body against the external environment. Cutaneous wound healing is a critical process to restore skin integrity after an injury, which requires a cascade of biological interactions involving cell differentiation, migration, proliferation, and remodeling [1-3]. Burn injury is a common cause of skin damage. Skin burn remains a major cause of high morbidity and mortality. A deep burn is unlikely to heal within 3 weeks and will heal with scarring [4]. Although novel biomaterials and biomedical devices have been applied in treating skin burn, the cure rate of most clinical applications remains 50%–60%. Therefore, it is necessary to develop novel approaches to accelerate damage repair

after burn injury.

Mesenchymal stem cells (MSCs) have considerable potential in regenerative medicine for their ability of renewal and differentiation into distinct cell types [5-9]. MSCs can be isolated from the bone marrow, umbilical cord, adipose tissues, and other adult tissues [9-11]. The easy availability of hucMSCs makes them a favourable candidate for injured tissue repair. hucMSCs are established to exhibit positive functional outcomes in various diseases [12]. Our previous studies have revealed that hucMSCs attenuate renal and hepatic injury in animal model [13-17]. In addition, hucMSC-derived exosomes (hucMSC-ex) displayed potent therapeutic

effects on a deep second-degree burn injury rat model and can control stem cells expansion after a regenerative response to prevent tissue from overcrowding by modulating YAP to orchestrate controlled cutaneous regeneration [18, 19]. Previous studies have reported that modified MSCs can play enhanced therapeutic roles in cardiac dysfunction and other diseases [20-23]. Small-molecule compounds have been particularly used as tools to manipulate stem cell fate and function [24, 25]. For modulating stem cell function, small-molecule compounds have several advantages, including the convenience in modifying their concentration, working duration, and rapid and reversible working effects [26].

DIM is a natural compound harvested from cruciferous vegetables, and it is the *in vivo* dimeric product of indole-3-carbinol (I3C), which belongs to the class of indole glucosinolate [27]. Both I3C and DIM have been reported to exert an antitumour property against various human cancers *in vitro* and *in vivo* by regulating cancer cell apoptosis and proliferation, cell cycle, the epigenetic status, and the key signalling pathways in tumour progression [28-30]. DIM has also been investigated for its potential in tissue injury repair, such as liver and acute lung injury [31, 32]. We previously demonstrated that a low level of DIM enhances the stemness of gastric cancer cells to promote tumour progression [33]. However, whether DIM can modify hucMSCs to improve their therapeutic effects on wound healing remains unknown.

In this study, we investigated the role of DIM in hucMSC modification for wound healing. We demonstrated that DIM induces exosomal Wnt11 autocrine signalling to activate β -catenin signalling and reinforces the stemness of hucMSCs. DIM-hucMSCs showed a desirable repairing ability in a deep second-degree burn injury rat model.

Materials and methods

All experimental protocols were approved by the Medical Ethics Committee of Jiangsu University (2012258).

Cell culture

HucMSCs were obtained from the affiliated hospital of Jiangsu University with the permission of mothers and were freshly processed within 6 h. HucMSCs were isolated as previously described [34] and maintained in a low-glucose Dulbecco's modified Eagle medium (DMEM) containing 10% foetal bovine serum (FBS; Bovogen Biologicals, South America). HaCAT cells were purchased from American Type Culture Collection and cultured in a high-glucose DMEM with 10% FBS. The culture medium was

changed every 2 days. Dermal fibroblasts (DFL) cells were isolated from rat back skin as previously described [18]. The cells were passaged every 3 or 4 days, and those passaged at 3-6 were used for additional studies.

Preparation of DIM-hucMSCs and the conditioned medium

DIM was dissolved in dimethyl sulfoxide (DMSO) to prepare a 500 mM solution and diluted in DMEM to the working concentration. The cells treated with 0.1% DMSO serving as the control. HucMSCs were treated with different concentrations of DIM for 48 h and subsequently collected for following experiments. For preparing the conditioned medium (CdM), the culture supernatant of the treated hucMSCs were discarded, and a fresh medium was added for an additional 48 h.

Rat skin wound model and treatment

The deep second-degree burn injury rat model was established as previously described [18]. After inducing burns at 80°C for 8 s, the wounds were administered immediate cell therapy by injecting 1×10^6 cells (with or without DIM) suspended in 200 μ L of phosphate-buffered saline (PBS) at three sites. The rats in the control group were injected with 200 μ L of PBS and were housed separately. Two weeks later, all the rats were sacrificed, and the injured area was analysed for further investigation.

Real-time reverse transcription polymerase chain reaction

The total RNA was isolated from hucMSCs and skin cells by using the Trizol reagent (Invitrogen). Two microgram aliquots of RNAs were synthesised according to the manufacturer's protocol (Vazyme). Real-time polymerase chain reactions (PCR) were performed using the QuantiTect SYBR Green PCR kit (Toyobo). The primer sequences are listed in Supplementary Table 1.

Western blot

The cells were lysed in a radioimmunoprecipitation assay buffer with proteinase inhibitors. An equal amount of protein samples was loaded and separated in a 12% sodium dodecyl sulfate polyacrylamide gel electrophoresis gel. Following electrophoresis, the proteins were transferred to a polyvinylidene fluoride membrane, subsequently blocked with 5% (w/v) nonfat milk, and incubated with primary antibodies at 4 ° C overnight. The primary antibodies were anti-Sox2 (Millipore, USA); anti-Oct4 (SAB, USA); anti-SALL4 (Abnova, USA); anti- β -catenin (Cell Signaling Technology, USA); anti-CK19 and anti-PCNA (Bioworld, USA);

anti-Wnt11 (Santa Cruz, USA); and anti-GAPDH (Kangcheng, China). After washing with Tris-buffered saline and Tween 20 for three times, the membranes were incubated with secondary antibodies (CWBI, China) at 37° C for 1 h. The target proteins were subsequently visualised using enhanced chemiluminescence.

Immunohistochemistry

Skin tissues were obtained from sacrificed rats and processed into paraffin sections (5-mm thick). Immunohistochemical staining was performed as previously described [35]. Furthermore, 1:50 and 1:100 dilutions were used for β -catenin primary antibody and proliferating cell nuclear antigen (PCNA), respectively. The secondary antibodies were purchased from Boster (Wuhan, China). The tissue sections were visualised with 3,3'-diaminobenzidine, counterstained with hematoxylin, and observed through high-power light microscopy (Nikon, Tokyo, Japan).

Osteogenic and adipogenic differentiation *in vitro*

HucMSCs and DIM-hucMSCs were seeded in 35-mm plates in an osteogenic differentiation medium (0.1 mM dexamethasone, 10 mM β -glycerophosphate, and 50 mg/L ascorbic acid) or adipogenic differentiation medium (Cyagen Biosciences, CA, USA) for 2 weeks, according to the manufacturer's instructions. After the induction, the osteogenic and adipogenic potential was evaluated through alizarin red and oil red O staining, respectively.

Lentiviral knockdown of Wnt11 in hucMSCs

A lentiviral expression vector containing the Wnt11 shRNA sequence (Sigma) was selected for targeting Wnt11; it was classified as Lenti-Wnt11 shRNA, and Lenti-GFP shRNA was used as the negative control vector. The Lenti-Wnt11 shRNA vectors were generated by ligating the vector Tet-pLKO-puro with Wnt11 shRNA oligonucleotides. The sequences of Wnt11 shRNA oligonucleotides were as follows: forward, 5'-CCGGCAGTGCAA CAAGACATCCAACCTCGAGTTGGATGTCTTGTTC CACTGCTTTTTG-3' and reverse, 5'-AATTCAAAA GCAGTGCAACAAGACATCCAACCTCGAGTTGGA TGTCTTGTTCAGTGC-3'. The sequences of the control shRNA were as follows: forward, 5'-CCGGCAAGCTGACCCTGAAGTTCATCTCGA GATGAACCTCAGGGTCACGTTGCTTTTTG-3' and reverse, 5'-AATTCAAAAAGCAAGCTGACCCTGA AGTTCATCTCGAGATGAACCTCAGGGTCACGTT GC-3'. A recombinant lentivirus was produced by cotransfecting HEK293T cells with PLKO-GFP

shRNA or PLKO-Wnt11 shRNA, PU1562, and PU1563 plasmids by using Lipofectamine 2000 (Invitrogen). The virus-containing supernatant was harvested at 48 h and 72 h post transfection. HucMSCs were transduced with the prepared lentivirus (Lenti-Wnt4 shRNA or Lenti-GFP shRNA) and selected with 1 μ g/mL of puromycin (Invitrogen) for 15 days. shRNA expression was induced by adding 80 μ g/mL of doxycycline. The efficiency of Wnt11 knockdown was evaluated through real-time quantitative reverse transcription (RT)-PCR and Western blot.

Luciferase reporter activity assay

The CdM of DMSO- and DIM-hucMSCs was prepared for the luciferase reporter activity assay. The TOP- or FOP-Flash luciferase reporter plasmid was cotransfected into HEK293T cells together with the Renilla luciferase gene, which is governed by the human β -actin promoter, to normalise the transfection efficiency. At 6 h post transfection, the prepared CdM was added and incubated for another 24 h. The cells were collected, and activities of both firefly and Renilla luciferases were quantified using the dual-luciferase reporter assay system (Promega). The Wnt reporter activity was determined using TOP-FOP luciferase.

Luminex assay

The concentrations of granulocyte-macrophage colony-stimulating factor (GM-CSF); interferon gamma; interleukin (IL)-6; IL-8; IL-10; IL-17a; interferon-inducible protein-10; monocyte chemotactic protein 1 (MCP-1); regulated on activation, normal T-cell expressed and secreted (RANTES); tumour necrosis factor- α ; and vascular endothelial growth factor (VEGF) in hucMSCs were measured using Luminex kits (Millipore), according to the manufacturer's instructions.

Isolation and characterization of exosomes

Exosomes were extracted from the CdM of DMSO- and DIM-hucMSCs. Extraction and purification were conducted as previously described [33]. The exosome-free CdM was collected and filtered through a 0.22- μ m filter, and the exosomes were stored at -80 °C. The protein content of the exosomes was detected using the bicinchoninic acid protein assay kit (CWBI, Shanghai, China). Furthermore, exosome morphology was identified through transmission electron microscopy (FEI Tecnai 12, Philips, Netherlands). The NanoSight LM10 system (NanoSight, Amesbury, UK) was used for exosome tracking, distribution, and particle number counting. The expression of CD9, CD63, and CD81, surface markers of exosomes, was determined through

Western blot.

Cell scratch assay

HaCAT cells were seeded at the density of 2×10^5 cells/well in six-well plates and incubated at 37°C in 5% CO_2 for 24 h to create confluent monolayers. The monolayers were scratched with a sterile pipette tip. To measure cell mobility, we obtained images from five random fields at 24 h after scratching. The width of the original scratch was calculated using the NIH Image programme (<http://rsb.info.nih.gov/nih-image/>). The migration ratio was calculated as follows: (the width of the original scratch – the width of the actual scratch)/the width of the original scratch $\times 100$.

Statistical analysis

All the data are shown as mean \pm standard deviation. The statistically significant differences between groups were assessed using analysis of variance or t test by using Prism software (GraphPad, San Diego, USA). $P < 0.05$ was considered statistically significant.

Results

DIM-hucMSCs exerted an improved impairing effect on wound healing in a rat deep second-degree burn injury model

To determine whether DIM modulates the therapeutic effects of hucMSCs on wound healing, we established a second-degree injury rat model and evaluated the impairing ability of DIM-hucMSCs at 2 weeks after cell transplantation (**Figure 1a**). We observed that both DMSO- and DIM-hucMSCs favourably healed the wounds (complete re-epithelialization in all the six wounds in the DIM-hucMSC group; five of the six wounds in the DMSO-hucMSC group) compared with the control treatment (complete re-epithelialization in one of the six wounds). However, the scabs in the DIM-hucMSC group had sloughed, and the new skin tissues were exposed. Only a sloughing tendency appeared in the hucMSC group (**Figure 1b**). Hematoxylin and eosin staining confirmed that the DIM-hucMSC treatment led to a more favourable impairing effect on the epidermis, dermis, and hair follicle than did the hucMSC treatment (**Figure 1c**). PCNA immunochemical staining revealed an increased number of PCNA-positive cells in both DMSO- and DIM-hucMSC groups, and the DIM-hucMSC group had more PCNA-positive cells than did the DMSO-hucMSC group (**Figure 1d**). The histological scores of the wounds were also considerably higher in the DIM-hucMSC group than in the DMSO-hucMSC and control groups (**Figure 1e** and **Supplementary**

Table 1). The relative expression of collagen I to collagen III reflects the scar formation potential. Real-time RT-PCR showed that collagen I:III expression was higher in the DMSO- and DIM-hucMSC groups than in the control group and was much higher in the DIM-hucMSC group (**Figure 1f**). Immunofluorescence staining showed that the expression of CK19, a marker of re-epithelialization, highly increased in the DIM-hucMSC group compared with that in the DMSO-hucMSC group (**Figure 1g**). β -Catenin activation is essential for wound healing [18]. Therefore, we detected β -catenin expression in wounded tissues through immunohistochemical staining. We demonstrated a higher number of β -catenin-positive cells in the DIM-hucMSC group (**Figure 1h**). In addition, the results revealed that 50 μM of DIM did not increase the growth and the stemness marker expression level of skin cells *in vitro* (**Figure S1a, b, c**) and showed no significant repair effect *in vivo* (**Figure S1d**), which excluded the possibility that DIM directly affected skin tissue recovery. Altogether, DIM-hucMSCs showed a more efficient impairing ability than did hucMSCs in wound healing *in vivo*.

DIM upregulated the stemness of hucMSCs

DIM has been reported to regulate stem cell function by inducing the expression of stemness transcription factors. To determine the mechanism underlying the improved therapeutic effects of DIM-hucMSCs on a deep second-degree burn injury, we detected the expression of stemness transcription factors through real-time RT-PCR and Western blot. We demonstrated that DIM can dose-dependently induce the expression of Oct4, Nanog, Sox2, and Sall4 in hucMSCs and that 50 μM of DIM exerts the strongest inducing effects on the expression of these factors (**Figure 2a, b**). Notably, we demonstrated that hucMSCs are more tolerant to DIM than gastric cancer cells. MTT assay was conducted to test the effect of DIM on the proliferation of gastric cancer cell lines SGC-7901, HGC-27, and hucMSCs for 48h (gastric cancer cell lines as control). The IC_{50} of DIM on three cell lines SGC-7901, HGC-27, hucMSC were calculated as 60.743 μM , 42.812 μM and 158.11 μM respectively (**Figure S2a**). Furthermore, 50 μM of DIM inhibited the expression of the stemness transcription factors in tumour cells, whereas it increased the expression of these factors in hucMSCs (**Figure S2b**). Immunofluorescent staining confirmed that 50 μM of DIM can enhance the expression of Oct4 and Sall4 in hucMSCs (**Figure 2c**). DIM-hucMSCs proliferated faster and formed more colonies than did DMSO-hucMSCs, indicating an increased

self-renewal and proliferation ability (Figure 2d). We next determined the differentiation potential of hucMSCs in each group and demonstrated an increased potential of DIM-hucMSCs to differentiate into adipocytes and osteoblasts in the appropriate CdM (Figure 2e). The expression of adiponectin and alkaline phosphatase (ALP), markers of adipocytes and osteoblasts, respectively, was consistently elevated in the DIM-hucMSC group (Figure 2f, g). The secretion of bioactive molecules is the main mechanism underlying the therapeutic effects of MSCs in tissue injury. We also evaluated the paracrine effects of DIM-hucMSCs and observed that the expression of multiple factors, including GM-CSF, IL-6, MCP-1, and VEGF, was considerably increased in DIM-hucMSCs (Figure S4). In summary, DIM enhanced the stemness of hucMSCs.

DIM enhanced the stemness of hucMSCs through β -catenin activation

The Wnt/ β -catenin signalling pathway is critically involved in regulating cell stemness[36]. We subsequently evaluated the activity of β -catenin in DIM-hucMSCs and observed that 50 μ M of DIM markedly upregulated the TOP-flash reporter activity in hucMSCs (Figure 3a). DIM concentration-dependantly increased the β -catenin level in hucMSCs (Figure 3b). Moreover, immunofluorescent staining confirmed an increased expression and nuclear translocation of β -catenin in 50 μ M DIM-treated hucMSCs (Figure 3c, d). To further verify the activation of Wnt/ β -catenin signalling and its role in

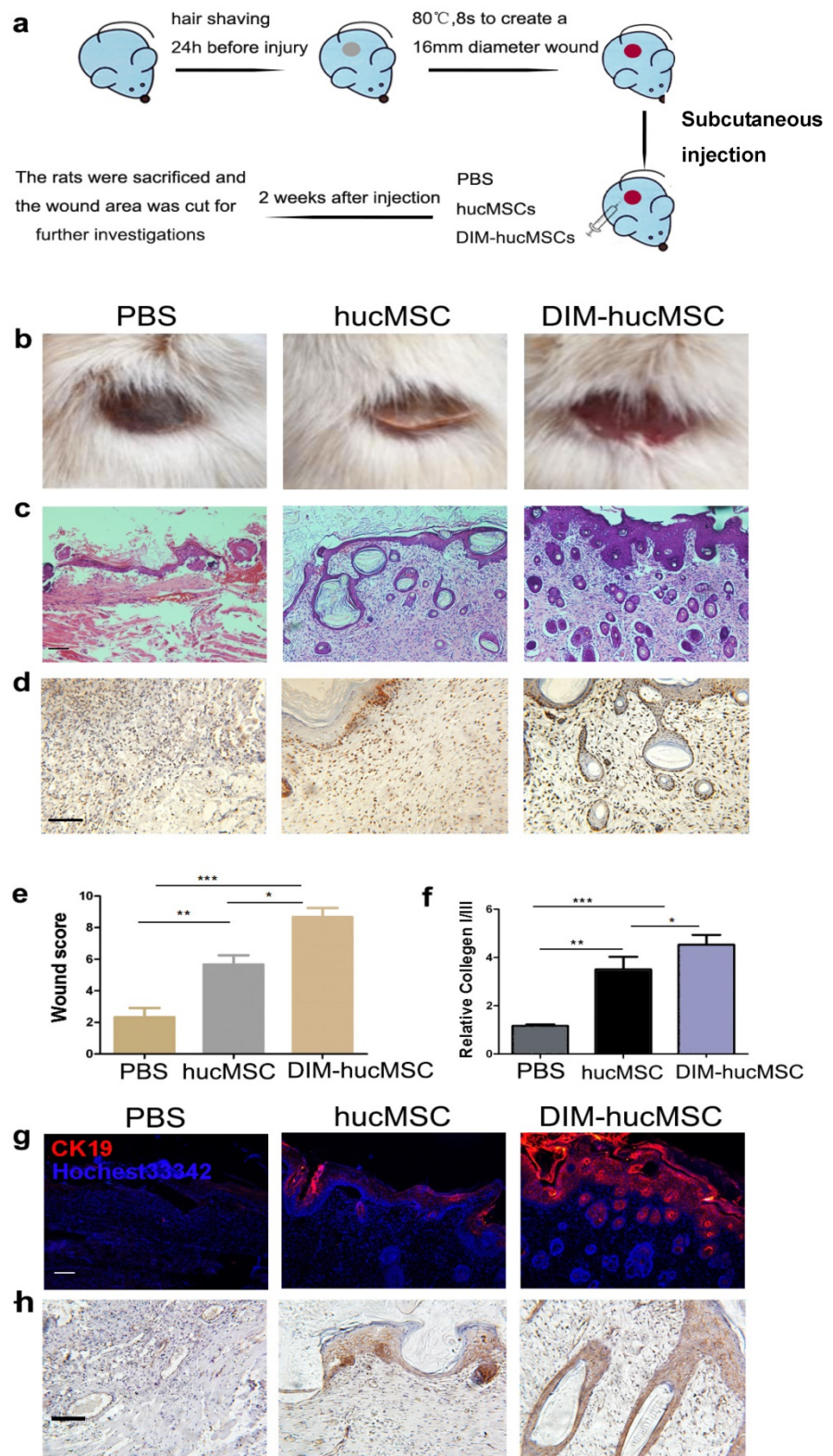


Figure 1. DIM-hucMSCs promoted cell proliferation and re-epithelialization in a rat deep second-degree burn injury model. (a): A schematic diagram showing the establishment of *in vivo* model. (b): General view of differently treated rats. (c): Representative micrographs of wound histological images (H & E stain) at 2 weeks after treatment. Scale bar = 100 μ m. (d) : Representative images of immunohistochemical staining of PCNA in each group (200 \times). (e): Wound histological scores were calculated at 2 weeks after the treatment (n = 6; * p < 0.05, ** p < 0.01, *** p < 0.001). (f): Quantitative analyses for the relative mRNA level of type I and III collagen in wound tissue at 2 weeks after treatment (n = 6; * p < 0.05, **p < 0.01, *** p < 0.001). (g): Representative immunofluorescence images of the CK19 expression in the injured area. (h): Representative images of immunohistochemical staining of β -catenin in each group (200 \times).

regulating the stemness of hucMSCs, we administered ICG001, a selective inhibitor of β -catenin-CREB-binding protein interaction, to block β -catenin activation, which did not affect the DIM-hucMSC cell viability under the condition of 50 μ M of DIM, 48h treatment (Figure S3). The inhibition of β -catenin reversed the DIM-induced enhancement of stemness. Moreover, 50 μ M of DIM upregulated the expression of β -catenin and its downstream target genes (cyclin D3 and CD44), which were also abrogated by a simultaneous treatment with ICG001 (Figure 3e, f). We subsequently determined the adipogenic and

osteogenic potential of hucMSCs in the presence or absence of ICG001. ICG001 significantly reduced the promoting role of DIM in adipogenesis and osteogenesis and expression of adiponectin and ALP in hucMSCs (Figure 3g, h). The colony formation assay revealed inhibitory effects of ICG001 on the DIM-induced proliferation of hucMSCs (Figure 3i). Moreover, ICG001 reversed the altered secretion of multiple factors in DIM-hucMSCs (Figure S4). These results indicate that DIM enhanced the stemness of hucMSCs by activating Wnt/ β -catenin signalling.

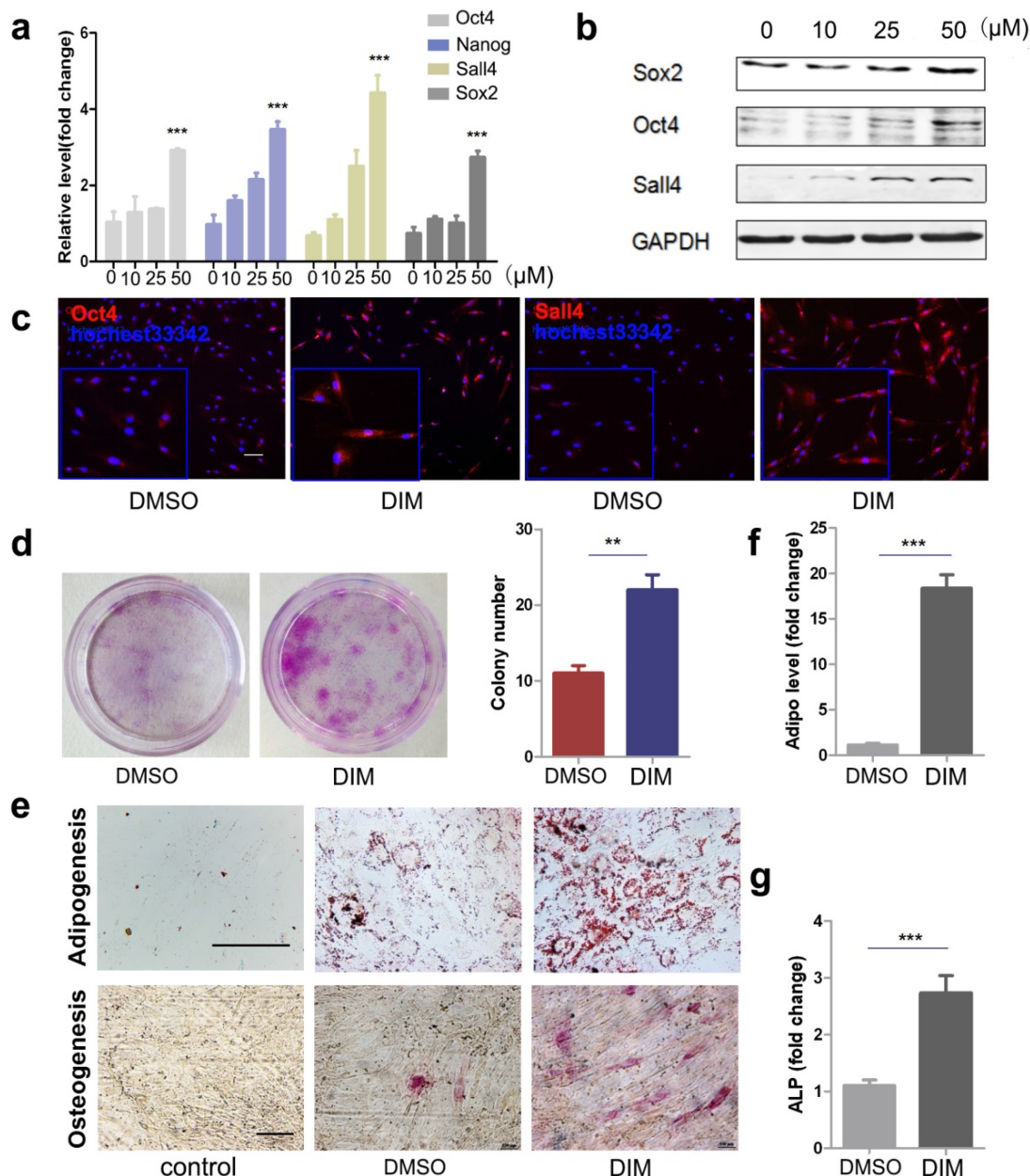


Figure 2. DIM upregulated the stemness of hucMSCs (a): HucMSCs were treated with DIM in a concentration gradient manner (0, 10, 25, 50 μ M) for 48 h. qRT-PCR for stemness transcription factors (n = 3; * p < 0.05, **p < 0.01, ***p < 0.001). **(b):** Western blot for Oct4, Sox2, Sall4 in differently treated hucMSCs. **(c):** Representative immunofluorescence images of Oct4 and Sall4 in hucMSCs after treatment with 50 μ M DIM for 48 h. **(d):** HucMSCs were treated with 50 μ M DIM and 0.1% DMSO, respectively, for 48 h. The cells were collected and seeded at 1000 cells to conduct a colony-forming assay. The cells were fixed and stained 10 days later. **(e):** Adipogenic differentiation and osteogenic differentiation of hucMSCs after treatment with 50 μ M DIM. **(f):** qRT-PCR for detecting adiponectin gene expression level (***p < 0.001). **(g):** qRT-PCR for detecting ALP gene expression detection (***p < 0.001).

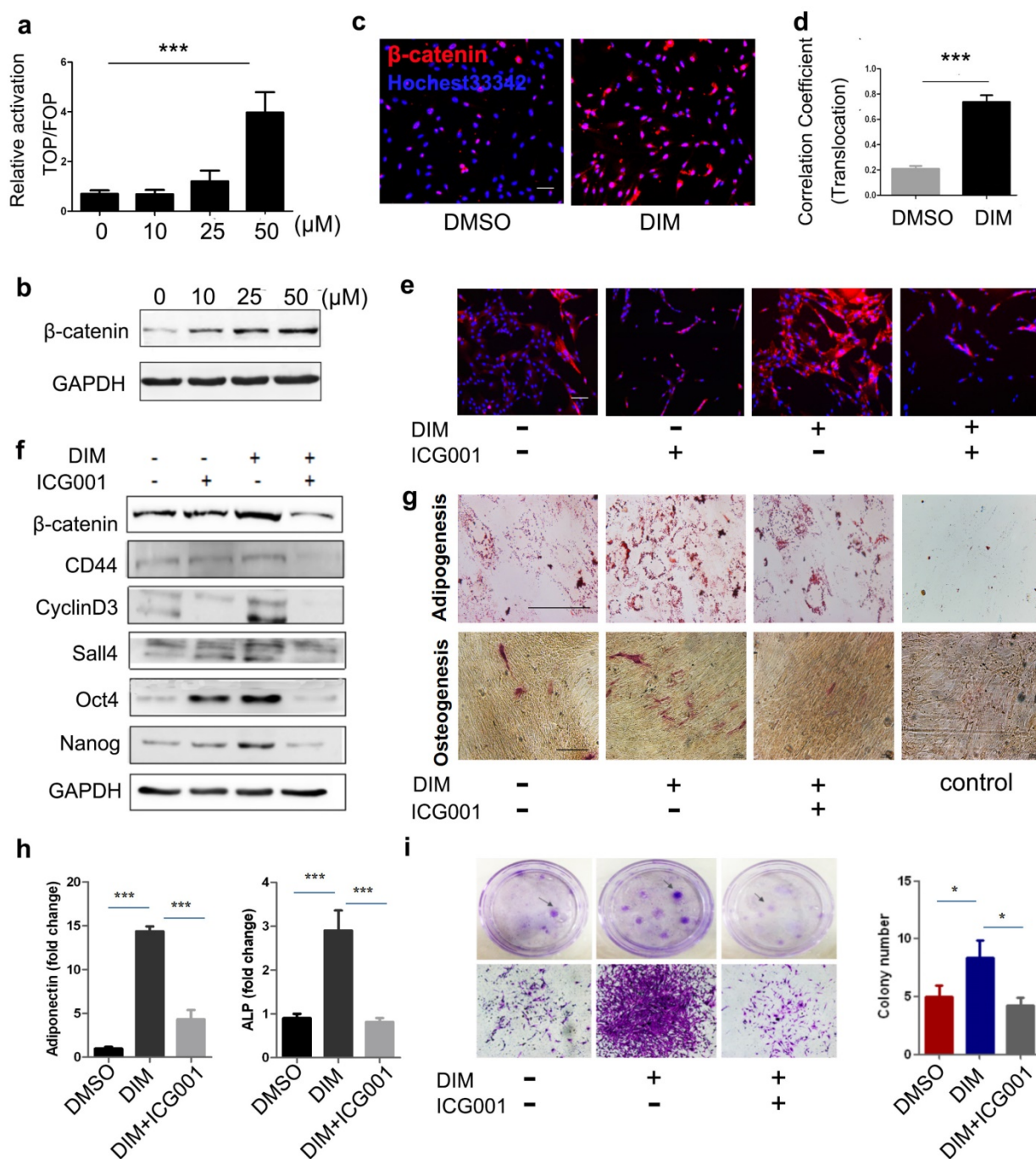


Figure 3. DIM-induced hucMSC stemness upregulation depended on Wnt/β-catenin activation (a): 293T cells transfected with the TOP- or FOP-Flash luciferase reporter were treated with the CdM from differently treated hucMSCs (0.1% DMSO and 10, 25, 50 μM DIM). The ratio between TOP- and FOP-Flash luciferase activity were determined at 24 h after treatment (n = 3, ***p < 0.001). **(b):** Western blot for β-catenin in differently treated hucMSCs. **(c,d):** The expression and translocation of β-catenin after 50 μM DIM treatment also detected through high content analysis. **(e):** HucMSCs were treated with 50 μM DIM in the presence or absence of ICG001 (20 μM/mL). The expression of β-catenin was detected by immunohistochemical staining. **(f):** Western blot for stemness transcription factors (Nanog, Oct4, and Sox2), β-catenin, and its downstream targets (cyclinD3 and CD44) in DIM-hucMSCs with or without ICG001 (20 μM/mL). **(g):** After 50 μM DIM treatment with or without ICG001 (20 μM/mL) for 48 h, hucMSCs were induced into osteogenic and adipogenic lineages in an appropriate medium. **(h):** qRT-PCR for the expression level of adiponectin and ALP (n = 3, ***p < 0.001). **(i):** Colony-forming assay for DIM-hucMSCs with or without ICG001 (20 μM/mL).

Inhibition of β-catenin activation reversed the improved repairing effects of DIM-hucMSCs on wound healing

To further clarify the role of DIM-induced β-catenin activation in the increased repairing effects

of hucMSCs on wound healing, we injected DIM-hucMSCs with or without ICG001 into the injured skin tissues. As expected, DIM-hucMSCs exhibited a decent recovery (complete re-epithelialization in all the six wounds) at 2 weeks after transplantation, whereas the ICG001 co-injection

group remained incompletely repaired with an inflammatory status (Figure 4a). The ICG001 co-injection group showed a relatively weak PCNA expression compared with the DIM-hucMSC group, indicating a reduced cell proliferation ability in the ICG001 co-injection group (Figure 4b). The histological scores in the ICG001 co-injection group were much lower than those in the DIM-hucMSC group and were comparable with those in the control group (Figure 4c). The relative expression of collagen I:III was decreased in the ICG001 co-injection group

compared with the DIM-hucMSC group, indicating a reduced scar formation potential (Figure 4d). The ICG001 cotreatment also downregulated the CK19 expression in the injured skin tissues (Figure 4e, f). Furthermore, the ICG001 cotreatment reversed the increased β -catenin expression in DIM-hucMSCs (Figure 4g). Altogether, the improved repairing effects of DIM-hucMSCs on wound healing was reversed by β -catenin inhibition, indicating that DIM upregulated the hucMSC stemness to promote wound healing through β -catenin activation.

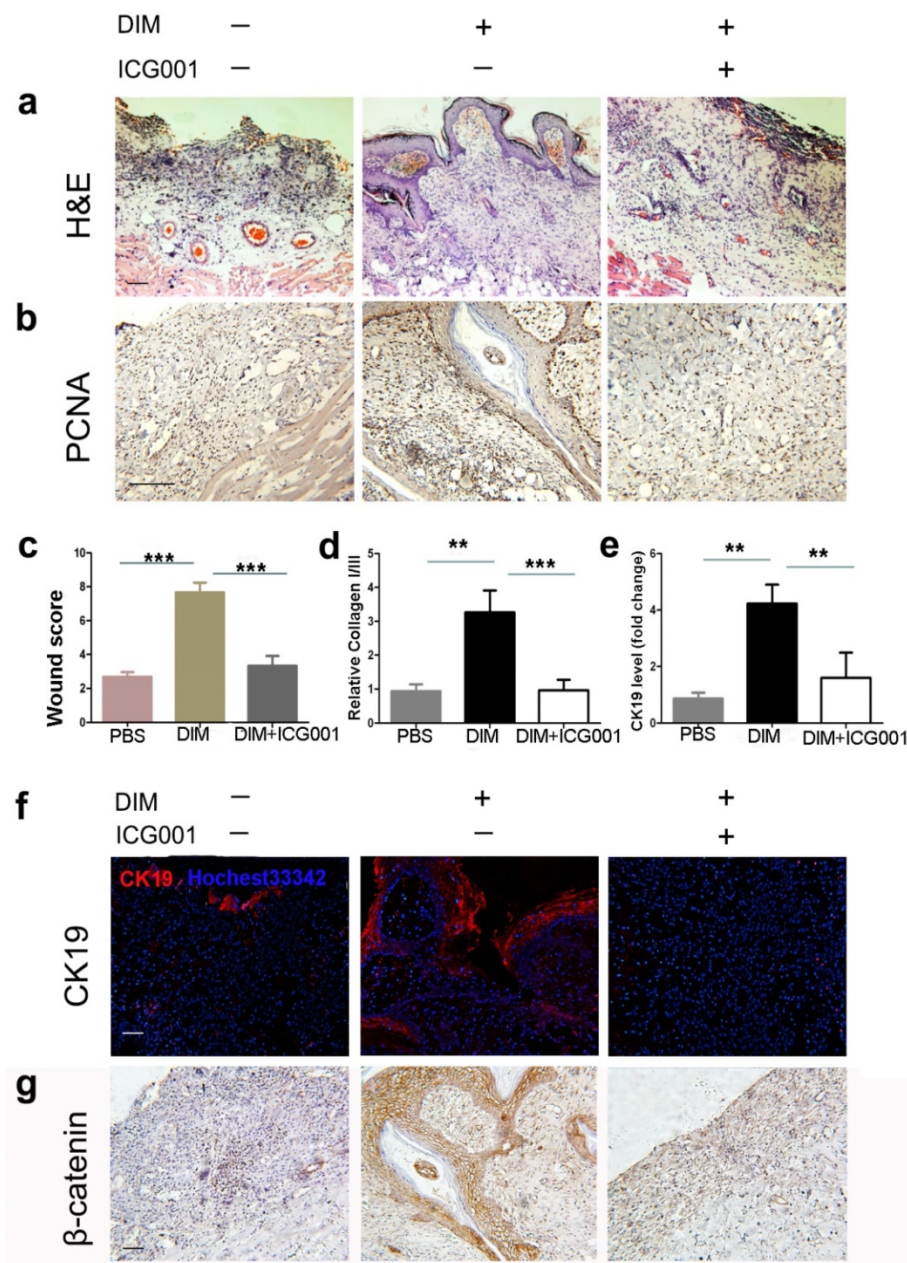


Figure 4. Inhibition of β -catenin reversed the recovery effects of DIM-hucMSCs in a rat deep second-degree burn injury model (a): The experimental rats were treated with PBS and DIM-hucMSCs with or without ICG001 (1 mg/rat). Representative micrographs of wound histological images (H&E stain) at 2 weeks after treatment. (b): Representative images of immunohistochemical staining of PCNA in each group (200 \times). (c): Wound histological scores were calculated at 2 weeks after treatment (n = 6; * p < 0.05, ** p < 0.01, *** p < 0.001). (d): Quantitative analyses for the relative mRNA level of type I and III collagen in wound tissues at 2 weeks after treatment (n = 6; * p < 0.05, ** p < 0.01, *** p < 0.001). (e): Quantitative analyses for the relative mRNA level of CK19. (f): Representative immunofluorescence images of CK19 expression in the wound area. Scale bar = 100 μ m. (g): Representative images of immunohistochemical staining of β -catenin in each group (200 \times).

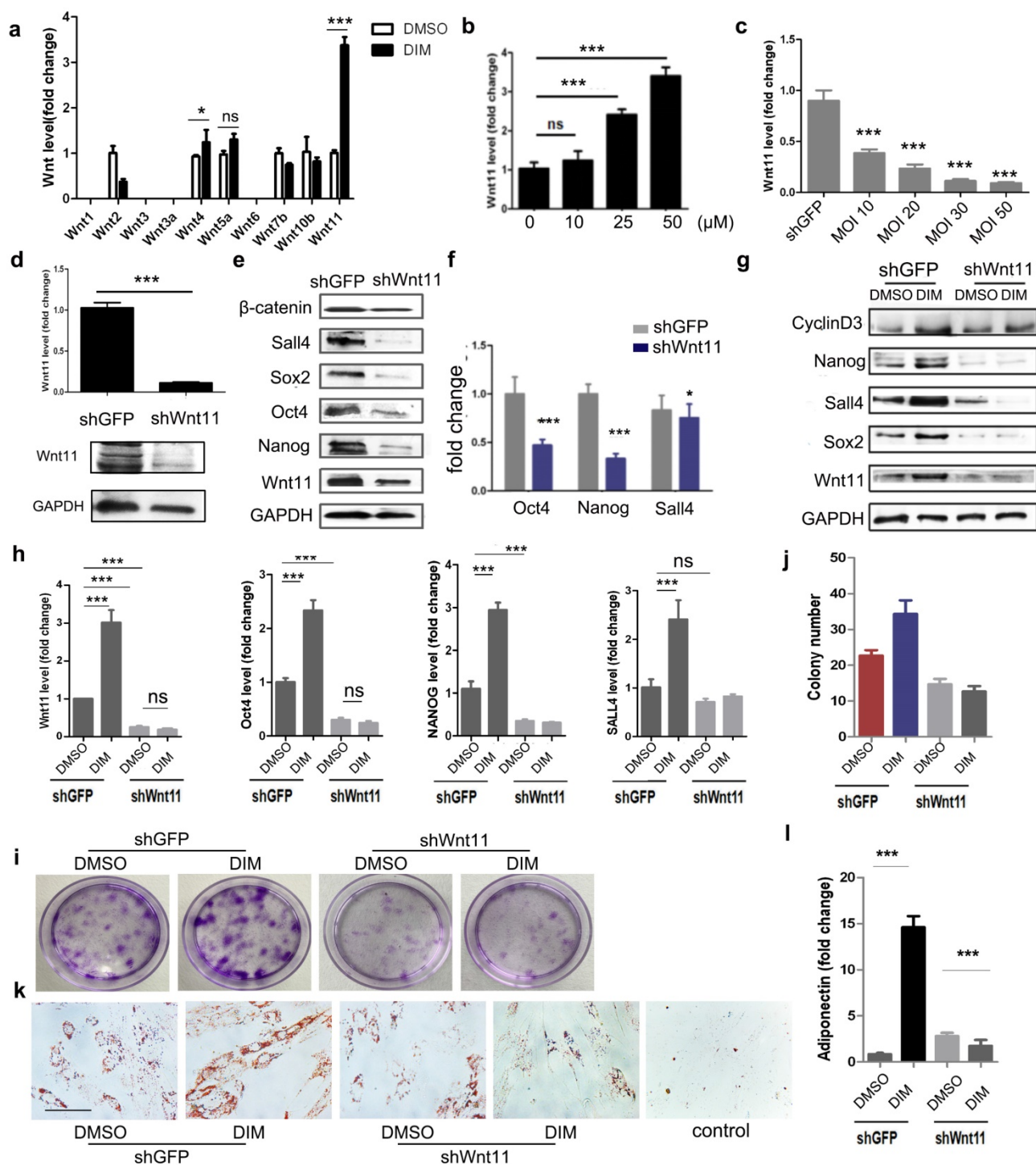


Figure 5. DIM induced β -catenin activation by Wnt11 (a): The mRNA levels of the Wnt family in DMSO-hucMSCs and DIM-hucMSCs through quantitative RT-PCR ($n = 3$, $^*p < 0.05$ and $^{***}p < 0.001$). **(b):** Quantitative analyses for the relative mRNA level of Wnt11 in differently treated hucMSCs (0.1%DMSO and 10, 25, and 50 μ M DIM for 48 h) ($n = 3$, $^{***}p < 0.001$). **(c):** qRT-PCR was used to select the most appropriate MOI of Wnt11-shRNA lentivirus and MOI30 was selected for having a high transfection efficiency and a low apoptosis of hucMSCs ($n = 3$, $^{***}p < 0.001$). **(d):** HucMSCs were transfected with Wnt11-shRNA (shWnt11) or GFP-shRNA lentivirus (shGFP), respectively. Wnt11 expression in hucMSCs were determined through qRT-PCR ($n = 3$, $^{***}p < 0.001$) and western blot. **(e):** Western blot for Wnt11, Nanog, Oct4, Sox2, Sall4, and β -catenin in shGFP-hucMSCs and shWnt11-hucMSCs. **(f):** qRT-PCR for the expression level of Nanog, Oct4, and Sall4 in shWnt11-hucMSCs and shGFP-hucMSCs ($n = 3$, $^*p < 0.05$ and $^{***}p < 0.001$). **(g):** shWnt11-hucMSCs and shGFP-hucMSCs were treated with 50 μ M DIM for 48 h and western blot for Wnt11, Sox2, Nanog, Sall4, and cyclinD3 and qRT-PCR. **(h):** for Oct4, Nanog, Sall4, and Wnt11 ($n = 3$, $^{***}p < 0.001$). **(i,j):** Representative images and colony numbers of colony formation in shGFP-hucMSCs and shWnt11-hucMSCs treated with 0.1% DMSO and 50 μ M DIM. Original magnification, 40 \times . **(k):** Adipogenic differentiation of shWnt11-hucMSCs and shGFP-hucMSCs were treated with 50 μ M DIM for 48 h. Original magnification, 400 \times . **(l):** qRT-PCR for adiponectin ($n = 3$, $^{***}p < 0.001$).

DIM induced β -catenin activation in hucMSCs through Wnt11

We subsequently determined the main factors responsible for DIM-induced β -catenin activation. We screened the expression of Wnt family members, including Wnt1, Wnt2, Wnt3, Wnt3a, Wnt4, Wnt5a, Wnt6, Wnt7b, Wnt10b, and Wnt11, in DIM-hucMSCs. The DIM treatment modified the expression of several Wnt molecules, of which Wnt11 showed the most significant increase. The expression of Wnt4, which markedly shares its sequence and activity with Wnt11 [37], also slightly increased after the DIM treatment (Figure 5a). Moreover, DIM dose-dependently increased the Wnt11 expression (Figure 5b). To substantiate the role of Wnt11 in DIM-hucMSCs, we knocked down Wnt11 by using shRNA and verified the efficiency by using both mRNA and protein levels (Figure 5c, d). Wnt11 knockdown led to a decreased expression of Oct4, Nanog, Sall4, and β -catenin, suggesting that Wnt11 acts as an upstream regulator of the canonical β -catenin signaling pathway (Figure 5e, f). Compared with the control knockdown cells (shGFP-hucMSCs), the Wnt11 knockdown hucMSCs (shWnt11-hucMSCs) treated with 50 μ M of DIM for 48 h showed a reduced expression of the stemness transcription factors (Figure 5g, h). Wnt11 knockdown also impaired the enhanced colony formation (Figure 5i, j) and adipogenic differentiation ability of DIM-hucMSCs (Figure 5k, l). Furthermore, Wnt11 overexpression led to an enhanced β -catenin expression as well as the Wnt reporter activity (Figure S5). Collectively, these results suggest that Wnt11 is critical for DIM-induced β -catenin activation and enhanced stemness of hucMSCs.

Wnt11 knockdown reversed the therapeutic effects of DIM-hucMSCs on wound healing

To assess the role of Wnt11 in the improved repairing effects of DIM-hucMSCs *in vivo*, we injected shWnt11-hucMSCs and shGFP-hucMSCs into the injured area in rats. The results revealed that Wnt11 knockdown led to a reduced effect on promoting re-epithelialization (Figure 6a). The number of PCNA-positive skin cells in the shWnt11-hucMSC group decreased compared with that in the shGFP group (Figure 6b). The wound scores in the shWnt11-hucMSC group were much lower than those in the shWnt11-hucMSC group (Figure 6c). The collagen I:III expression was decreased (Figure 6d), and the CK19 expression was significantly reduced in the

shWnt11-hucMSC group (Figure 6e, f). Immunohistochemical staining revealed that the DIM-induced increase of β -catenin expression was abrogated in the wounds in the shWnt11-hucMSC group (Figure 6g). In summary, Wnt11 knockdown reversed the improved therapeutic effects of DIM-hucMSCs on wound healing.

Wnt11 was transported by exosomes in an autocrine manner

We previously reported that exosomes mediated wound healing through Wnt4 transportation. Considering the low solubility of Wnt11 [37], we determined whether DIM induced Wnt11 expression in exosomes. First, we analysed the CdM of DIM-hucMSCs and observed that it can upregulate the expression of the stemness transcription factors in hucMSCs (Figure 7a, b). The CdM of DIM-hucMSCs can also enhance the colony-forming ability of hucMSCs (Figure 7c). Enzyme-linked immunosorbent assay (ELISA) showed elevated Wnt11 expression in the CdM of DIM-hucMSCs (Figure 7d). We further extracted the exosomes from DMSO- and DIM-hucMSCs, which were termed as DMSO-ex and DIM-ex, respectively. The NanoSight LM10 system was used for exosome tracking, size detection, and particle number counting (Figure S6). No difference was observed in the morphology or particle numbers between two types of exosomes after the DIM treatment. Both DMSO-ex and DIM-ex were 100-nm spherical vesicles; had a comparable particle number; and expressed CD9, CD63, and CD81 (Figure 7e). Exosomes derived from DIM-hucMSCs showed an increased expression of Wnt11, indicating that the DIM treatment affected the content of hucMSC-derived exosomes. We subsequently compared the expression of Wnt11 in exosomes and an exosome-free CdM (ex-free CdM) by using ELISA. DIM promoted Wnt11 secretion in exosomes. Moreover, exosomes showed a relatively higher level of Wnt11 expression than did ex-free CdM, indicating that Wnt11 was mainly present in exosomes rather than in ex-free CdM (Figure 7f). Compared with DMSO-ex, DIM-ex highly enhanced the colony formation and migration of skin cells. However, ex-free CdM from DIM-hucMSCs only showed slightly promoting roles (Figure 7g). These results suggest that DIM induce Wnt11 expression in exosomes in an autocrine manner.

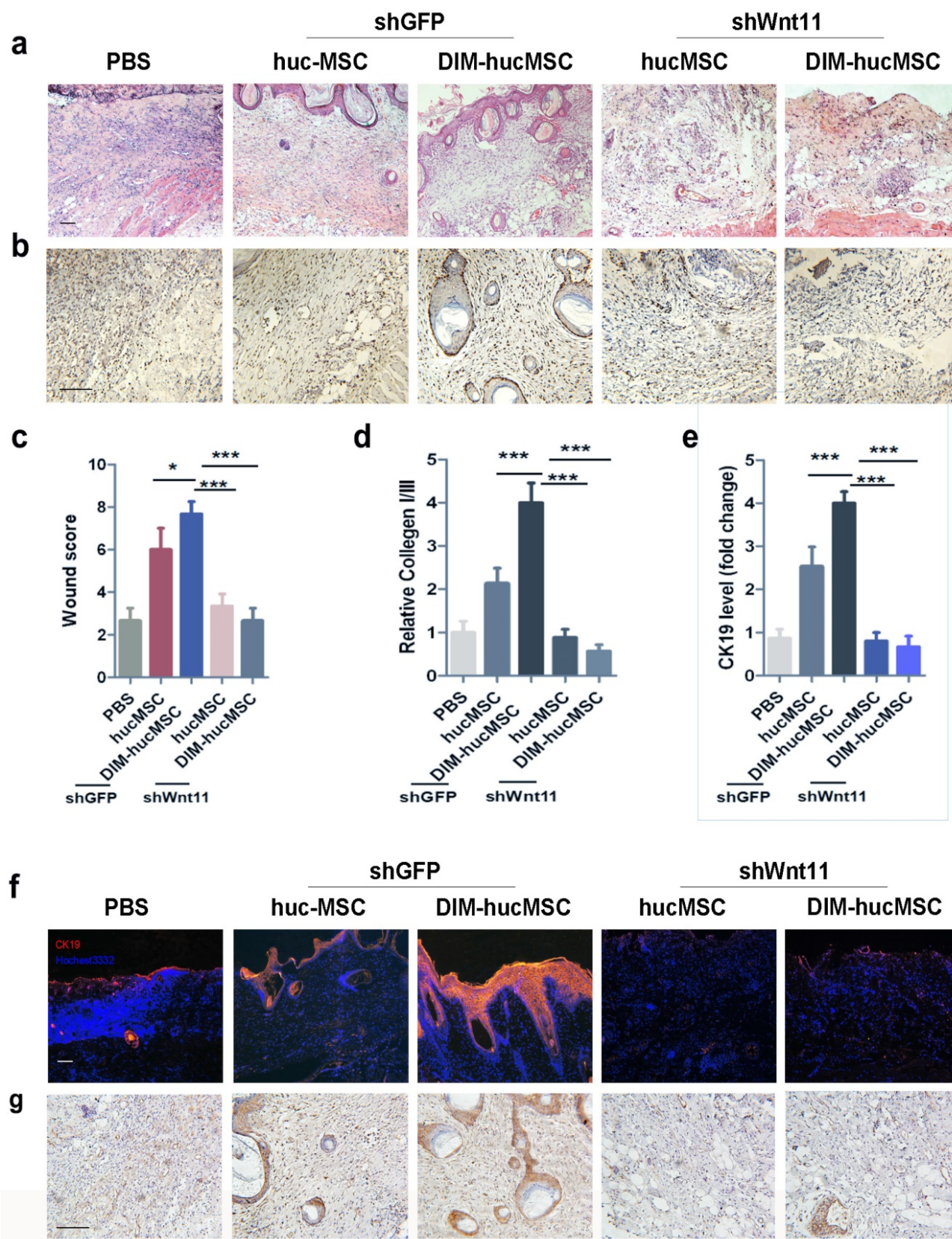


Figure 6. Wnt11 knockdown reversed the improved therapeutic effects of DIM-hucMSCs on wound healing (a): The rat model was subcutaneously injected with shGFP-hucMSCs, shGFP-DIM-hucMSCs, shWnt11-hucMSCs, and shWnt11-DIM-hucMSCs. The wound was subjected to H&E staining after 2 weeks of treatment. (b): Immunohistochemical staining for PCNA expression at 2 weeks of treatment (200×). (c): Wound histological scores (n = 6 at 2 weeks after treatment; *** p < 0.001). (d): Quantitative analyses for the relative mRNA level of CK19 in wound tissues at 2 weeks after treatment (n = 6; * p < 0.05, ** p < 0.01, *** p < 0.001). (e): Quantitative analyses for the relative mRNA level of type I and III collagen in wound tissues at 2 weeks after treatment (n = 6; * p < 0.05, ** p < 0.01, *** p < 0.001). (f): Representative immunofluorescence images of CK19 expression in the injured area. (g): Representative images of immunohistochemical staining of β-catenin in each group (200×).

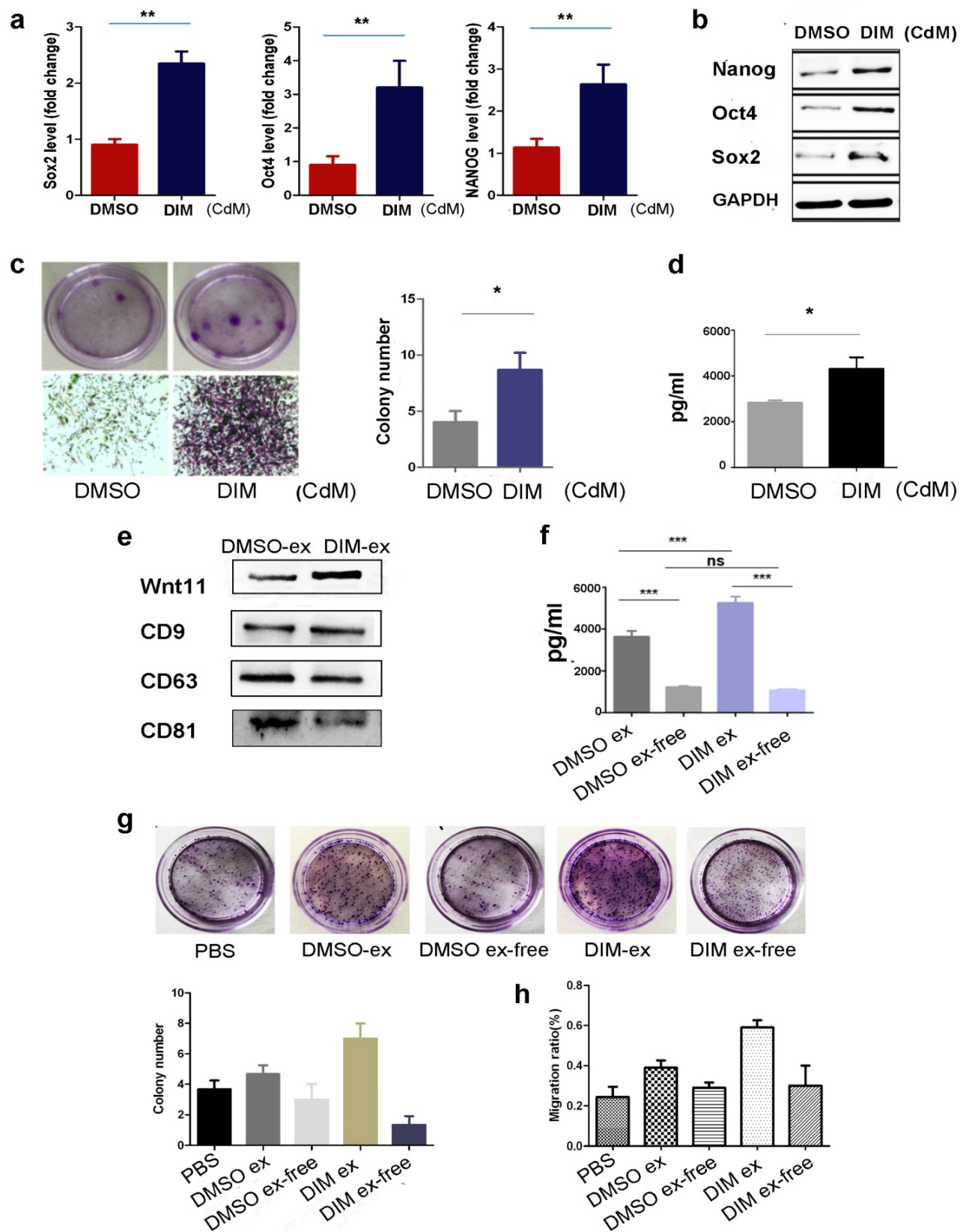


Figure 7. Wnt11 was transported by exosomes in an autocrine manner (a): HucMSCs were treated with 50 μ M of DIM for 48 h, and the CdM was prepared. HucMSCs were subsequently treated with a different CdM for 48 h. Quantitative analyses were conducted for assessing the relative mRNA level of Sox2, Oct4, and Nanog (n = 6; **p < 0.01). **(b):** Western blot for Oct4, Sox2, Nanog in differently treated hucMSCs. **(c):** The colony forming assay of hucMSCs treated with a different CdM. **(d):** ELISA to detect the expression level of Wnt11 in hucMSCs and DIM-hucMSC-derived exosomes (n = 6; *p < 0.05). **(e):** Western blot for the expression of Wnt11 in hucMSC and DIM-hucMSC-derived exosomes. **(f):** ELISA to detect the expression level of Wnt11 in hucMSCs, DIM-hucMSC-derived exosomes, and the exosome-free CdM (n = 6; ***p < 0.001). **(g):** HaCAT cells were treated with 200 μ g exosome-derived from hucMSCs and DIM-hucMSCs and the exosome-free CdM. The colony-forming assay was conducted to detect the proliferative capacity of HaCAT cells. **(h):** HaCAT cells were treated as described in **(g)**, and the cell migration capacity was detected using the cell scratch assay.

Discussion

Burn injury treatments have always been an intractable medical problem. The therapeutic methods so far are function-limited. For instance, biofilms easily lead to a wound infection and initiate an inflammatory response. Skin grafts can reduce deaths from infection. However, such injuries are long-lasting and many patients suffer from chronic pain for a long time [39, 40]. Cell-based therapies and tissue regeneration are new approaches to overcome the present limitations of burn wound healing. Functionally and phenotypically identical cells are generated to replace cells lost to disease and injury; they would have better specificity compared to conventional therapeutics by producing a supply of immunologically tolerant cells or tissue, leading to a permanent recovery for damaged tissues [26].

MSCs are excellent candidates in cell-based therapy for their promoting roles in tissue repair, particularly in skin burn injury, by increasing angiogenesis, extracellular matrix (ECM) production and remodeling, differentiation of MSCs into endothelial cells (EC), pericytes (PC), fibroblasts and keratinocytes, and also the secretion of exosomes [41]. The maintenance of stemness is also related to the rapidly growing, multidirectional differentiation, and paracrine abilities of MSCs, which allows them to facilitate wound healing. The secretion of a broad range of bioactive molecules is now considered to be the main mechanism by which MSCs achieve their therapeutic effect. The loss of stemness, such as ageing, may cause a declined paracrine of VEGF, placental growth factor, and hepatocyte growth factor in stem or progenitor cells and an attenuation of their regenerative potential in cardiovascular diseases and osteoarthritis [42-44]. In the present study, we demonstrated that DIM could improve the stemness of hucMSCs and enhance their proliferation, differentiation, and paracrine abilities. The blockade with ICG001 reduced the secretion of the paracrine factors in DIM-hucMSCs, suggesting that DIM enhances the stemness of hucMSCs to make them more powerful and helpful MSCs in improving their repairing efficiency.

As for the DIM treated MSCs, there is an increasing interest exists about the role of small molecule drugs in modulating the stem cell fate and function. Chemical approaches will play leading roles in guiding therapeutic developments in regenerative medicine [26]. Enabling and improving the generation of cells as well as enhancing their functions by chemical approaches will undoubtedly expand cell-based therapies to address many medical needs. Small molecule drugs are more convenient for

providing a rapid and reversible effects by altering their working concentration, duration time, and compositions [26]. Small molecule compounds have been widely used in the generation of induced pluripotent stem cells (iPSCs) [36, 45], which has shown predominance in regenerative medicine, such as Parkinson disease and sickle cell anaemia [46, 47]. The anticancer drug OHTM could replace some of the Yamanaka factors to generate iPSCs, resulting in safer therapies [48]. Moreover, human-induced pluripotent stem cell-derived MSCs have shown a more satisfactory alleviation of heart failure, less cardiomyocyte apoptosis, and fibrosis than naive MSCs in anthracycline-induced cardiomyopathy [20]. In addition, the pharmacological priming with ISX1, a 3,5-disubstituted isoxazoles, could enhance the myocardiocyte differentiation ability of adipose-derived stem cells and the persistence of exogenously transplanted cells to alleviate the impaired cardiac function [48]. The pretreatment of adipose-derived stem cells with curcumin before transplantation also facilitates myocardial recovery through antiapoptosis and angiogenesis [49, 50]. These studies indicate that stem cells can be modified to achieve more desirable repairing effects, and small molecule drugs have proven to be potential candidates for stem cell manipulation in regenerative medicine.

DIM is widely reported for its anti-tumour activity. The role of DIM in stem cell manipulation has not been characterised. 50 μ M of DIM can inhibit the growth and expression of stemness transcription factors of gastric cancer cells. However, it promotes the growth of hucMSCs and increases the expression of stemness transcription factors, suggesting that stem cells are more tolerant to anticancer drugs, making them potential candidates for pharmacological manipulation. Studies on the crossover of MSCs with chemicals, such as DIM, would supply a potential therapeutic strategy and benefit the regenerative medicine [26].

Wnt proteins are divided into two classes according to their biological activities. The Wnt1/Wg class includes Wnt1, Wnt3, Wnt3a, and Wnt8, which represent the canonical Wnts activating the Wnt/ β -catenin pathway; the Wnt5a class includes Wnt4, Wnt5a, Wnt5b, and Wnt11 that represent the noncanonical Wnts activating the Wnt/calcium and Wnt/JNK (PCP) pathways [37, 45]. Kestler *et al.* demonstrate that both canonical and noncanonical Wnts have the potential to activate all the pathways [51]. Wnt11 is associated with the canonical Wnt receptor LRP6 to activate the β -catenin pathway. Furthermore, the Wnt11 promoter contains two conserved TCF/LEF binding sites, suggesting that

β -catenin signals can directly regulate Wnt11 transcription [52, 53]. The depletion of Wnt11 reduces the activity of β -catenin [54]. In this study, we demonstrated that DIM induced Wnt11 expression to activate Wnt/ β -catenin signalling, leading to enhanced stemness in hucMSCs. Our findings are in accordance with the crosstalk between canonical and noncanonical Wnt/ β -catenin pathways. In addition, we demonstrated that Wnt11 knockdown can reverse the increased repairing effects of hucMSCs through DIM, indicating that Wnt11 is crucial for DIM-induced promoting role of hucMSCs in wound healing.

Exosomes are bioactive vesicles released by multiple cell types into the extracellular space. Exosomes act as transporters in cell-cell communication to deliver the message from their original cells to the recipient cells. The contents in exosomes include lipids, nucleic acids (DNA, mRNA, miRNA, and noncoding RNAs) and active proteins [55]. Wnt11 is a low soluble molecule, which requires post-translational modifications. Wnt is transferred by binding to the exosomal protein and exosomes are suggested as carriers for Wnt secretion and extracellular traveling [56, 57]. Wnts cannot be detected in exosome-free conditioned media of either mammalian or *Drosophila* cells [57-60]. Moreover, Wnt11 has been reported to participate in interfollicular epidermal stem cell self-renewal in an autocrine manner [36, 61]. In this study, we provided evidence that exosomes act as crucial transporters of Wnt11 in hucMSCs, and DIM can increase the secretion of exosomal Wnt11 to activate the Wnt/ β -catenin pathway in an autocrine manner. Furthermore, increasing evidence of the therapeutic potential of exosomes in several diseases has emerged, including kidney disease, cardiac disease, skin injury. With respect to skin wound healing, HucMSC-exosome mediated -Wnt4 signaling is required for cutaneous wound healing [18]. Guo *et al.* also reported that Exosomes derived from platelet-rich plasma promote the re-epithelization of chronic cutaneous wounds via activation of YAP in a diabetic rat model [62]. These findings strongly support the therapeutic potential of MSC-derived exosomes. To enhance the therapeutic effects of MSC-derived exosomes, it will be possible to modify the exosomes. Whether our DIM-hucMSC derived exosomes would have such better repairing effect and the potential mechanisms are interesting research deserve further investigations.

In summary, our findings indicate that DIM, a natural small molecule compound, can enhance the stemness of hucMSCs through exosomal Wnt11 autocrine to mediate Wnt/ β -catenin activation and

eventually improve the repairing ability of hucMSCs in wound healing.

Supplementary Material

Supplementary figures and tables.

<http://www.thno.org/v07p1674s1.pdf>

Acknowledgments

This study was supported by the National Natural Science Foundation of China (81572075), the Natural Science Foundation of the Jiangsu Province (BK20141303), Jiangsu Province for Outstanding Sci-tech Innovation Team in Colleges and Universities (Grant no. SJK2013-10), Jiangsu Province's Outstanding Medical Academic Leader and Sci-tech Innovation Team Programme (Grant no. LJ201117), Jiangsu Province's Major Project in Research and Development (BE2015667, BE2016717), the Innovation Project for Graduate Student Research of Jiangsu Province (Grant No. KYLX15_1096), the Priority Academic Programme Development of Jiangsu Higher Education Institutions, and China Postdoctoral Science Foundation Funded Project (Grant No. 2016M6000383).

Competing Interests

The authors have declared that no competing interest exists.

References

- Martin P. Wound healing--aiming for perfect skin regeneration. *Science*. 1997;276:75-81.
- Kirby GT, Mills SJ, Cowin AJ *et al.* Stem cells for cutaneous wound healing. *BioMed Res Int*. 2015;[Epub ahead of print].
- Ojeh N, Pastar I, Tomic-Canic M, *et al.* Stem cells in skin regeneration, wound healing, and their clinical applications. *Int J Mol Sci*. 2015;16:25476-25501.
- Cuttle L, Kempf M, Phillips GE, *et al.* A porcine deep dermal partial thickness burn model with hypertrophic scarring. *Burns*. 2006;32:806-820.
- Parenteau NL, Rosenberg L, Hardin YJ. The engineering of tissues using progenitor cells. *Curr Top Dev Biol*. 2004;64:101-139.
- Barry FP, Murphy JM. Mesenchymal stem cells: clinical applications and biological characterization. *Int J Biochem Cell*. 2004;36:568-584.
- Verfaillie CM. Adult stem cells: assessing the case for pluripotency. *Trends Cell Biol*. 2002;12:502-508.
- S CM. Exploring the development potential of adult somatic cells. *Chin Sci Bull*. 2001; 46:1
- Detamore MS. Human umbilical cord mesenchymal stromal cells in regenerative medicine. *Stem Cell Res Ther*. 2013;4:142.
- Jiang Y, Jahagirdar BN. Pluripotency of mesenchymal stem cells derived from adult marrow. *Nature*. 2002;418:41-49.
- Jackson L, Jones DR, Scotting P. Adult mesenchymal stem cells: differentiation potential and therapeutic applications. *J Postgrad Med*. 2007;53:121-127.
- Fan CG, Zhang QJ, Zhou JR. Therapeutic potentials of mesenchymal stem cells derived from human umbilical cord. *Stem Cell Rev*. 2011;7:195-207.
- Peng X, Xu H, Zhou Y, *et al.* Human umbilical cord mesenchymal stem cells attenuate cisplatin-induced acute and chronic renal injury. *Eep Biol Med*. 2013;238:960-970.
- Cao H, Qian H, Xu W, *et al.* Mesenchymal stem cells derived from human umbilical cord ameliorate ischemia/reperfusion-induced acute renal failure in rats. *Biotechnol Lett*. 2010;32:725-732.
- Chen Y, Qian H, Zhu W, *et al.* Hepatocyte growth factor modification promotes the amelioration effects of human umbilical cord mesenchymal stem cells on rat acute kidney injury. *Stem Cells Dev*. 2011;20:103-113.
- Qian H, Yang H, Xu W, *et al.* Bone marrow mesenchymal stem cells ameliorate rat acute renal failure by differentiation into renal tubular epithelial-like cells. *Int J Mol Med*. 2008;22:325-332.
- Yan Y, Xu W, Qian H, *et al.* Mesenchymal stem cells from human umbilical cords ameliorate mouse hepatic injury in vivo. *Liver Int*. 2009;29:356-365.

18. Zhang B, Wang M, Gong A, et al. HucMSC-exosome mediated-Wnt4 signaling is required for cutaneous wound healing. *Stem Cells*. 2015; 33:2158-2168.
19. Zhang Y, Liang X, Liao S, et al. Potent paracrine effects of human induced pluripotent stem cell-derived mesenchymal stem cells attenuate doxorubicin-induced cardiomyopathy. *Sci Rep*. 2015;5:11235.
20. Zhang B, Shi Y, Gong A, et al. HucMSC Exosome-Delivered 14-3-3 ζ Orchestrates Self-control of the Wnt Response via Modulation of YAP during Cutaneous Regeneration. *Stem Cells*. 2016;34(10):2485-2500.
21. Baksh D, Yao R, Tuan RS. Comparison of proliferative and multilineage differentiation potential of human mesenchymal stem cells derived from umbilical cord and bone marrow. *Stem Cells*. 2007;25:1384-1392.
22. Rachakatla RS, Pyle MM, Ayuzawa R, et al. Combination treatment of human umbilical cord matrix stem cell-based interferon-beta gene therapy and 5-fluorouracil significantly reduces growth of metastatic human breast cancer in SCID mouse lungs. *Cancer Invest*. 2008;26:662-670.
23. Rachakatla RS, Marini F, Weiss ML, et al. Development of human umbilical cord matrix stem cell-based gene therapy for experimental lung tumors. *Cancer Gene Ther*. 2007;14:828-835.
24. Schugar RC, Robbins PD, Deasy BM. Small molecules in stem cell self-renewal and differentiation. *Gene Ther*. 2008;15:126-135.
25. Xu Y, Shi Y, Ding S. A chemical approach to stem-cell biology and regenerative medicine. *Nature*. 2008;453:338-344.
26. Li W, Li K, Wei W. Chemical approaches to stem cell biology and therapeutics. *Cell Stem Cell*. 2013;13:270-283.
27. Maruthanila VL, Poornima J, Mirunalini S. Attenuation of carcinogenesis and the mechanism underlying by the influence of indole-3-carbinol and its metabolite 3,3'-diindolylmethane: a therapeutic marvel. *Adv Pharm Sci*. 2014;2014:832161.
28. Bonnesen C, Eggleston IM, Hayes JD. Dietary indoles and isothiocyanates that are generated from cruciferous vegetables can both stimulate apoptosis and confer protection against DNA damage in human colon cell lines. *Cancer Res*. 2001;61:6120-6130.
29. Li Y, Wang Z, Kong D, et al. Regulation of FOXO3a/beta-catenin/GSK-3beta signaling by 3,3'-diindolylmethane contributes to inhibition of cell proliferation and induction of apoptosis in prostate cancer cells. *J Bio Chem*. 2007;282:21542-21550.
30. Ali S, Banerjee S, Ahmad A, et al. Apoptosis-inducing effect of erlotinib is potentiated by 3,3'-diindolylmethane in vitro and in vivo using an orthotopic model of pancreatic cancer. *Mor Cancer Ther*. 2008;7:1708-1719.
31. Busbee PB, Nagarkatti M, Nagarkatti PS. Natural indoles, indole-3-carbinol (I3C) and 3,3'-diindolylmethane (DIM), attenuate staphylococcal enterotoxin B-mediated liver injury by downregulating miR-31 expression and promoting caspase-2-mediated apoptosis. *Plos One*. 2015; [Epub ahead of print].
32. Elliott DM, Nagarkatti M, Nagarkatti PS. 3,3'-diindolylmethane ameliorates staphylococcal enterotoxin B-induced acute lung injury through alterations in the expression of microRNA that target apoptosis and cell cycle arrest in activated T cells. *J Pharmacol Exp Ther*. 2014;350(2):341-352.
33. Zhu Y, Zhang B, Gong A, et al. Anti-cancer drug 3,3'-diindolylmethane activates Wnt4 signaling to enhance gastric cancer cell stemness and tumorigenesis. *Oncotarget*. 2016;7:16311-16324.
34. Zhou Y, Xu H, Xu W, et al. Exosomes released by human umbilical cord mesenchymal stem cells protect against cisplatin-induced renal oxidative stress and apoptosis in vivo and in vitro. *Stem Cell Res Ther*. 2013;4:34.
35. Zhang X, Xu W, Qian H, et al. Mesenchymal stem cells modified to express lentivirus TNF-alpha Tumorstatin(45-132) inhibit the growth of prostate cancer. *J Cell Mol Med*. 2011;15:433-444.
36. Lim X, Tan SH, Koh WL, et al. Interfollicular epidermal stem cells self-renew via autocrine Wnt signaling. *Science*. 2013;342:1226-1230.
37. Uysal OP, Kypsta RM. Wnt11 in 2011 - the regulation and function of a non-canonical Wnt. *Acta Physiol*. 2012;204:52-64.
38. Chen L, Xing Q, Zhai Q, et al. Pre-vascularization enhances therapeutic effects of human mesenchymal stem cell sheets in full thickness skin wound repair. *Theranostics*. 2017;7:117-131.
39. Oryan A, Alemzadeh E, Moshiri A. Burn wound healing: present concepts, treatment strategies and future directions. *J Wound Care*. 2017 Jan 2;26(1):5-19.
40. Subhamoy D, Aaron BB. Biomaterials and Nanotherapeutics for Enhancing Skin Wound Healing. *Front Bioeng Biotechnol*. 2016 ; 31(4):82.
41. Seiichiro M, Osamu I. Mesenchymal stem cells: The roles and functions in cutaneous wound healing and tumor growth. *J Dermatol Sci*. 2016; 16:30721-30726.
42. Efimenko AY, Kochegura TN, Akopyan ZA et al. Autologous Stem Cell Therapy: How Aging and Chronic Diseases Affect Stem and Progenitor Cells. *Bio Res*. 2015;4:26-38.
43. Efimenko AY, Dzhoyashvili NA, Kalinina NI. Adipose-derived stromal cells from aged patients with coronary artery disease keep MSC properties but exhibit age markers and have an impaired angiogenic potential. *Stem Cells Transl Med*. 2014; 3:32-41.
44. Maredziak M, Marycz K, Tomaszewski KA. The Influence of Aging on the Regenerative Potential of Human Adipose Derived Mesenchymal Stem Cells. *Stem Cells Int*. 2016;[Epub ahead of print].
45. Snippet HJ, Haegerbarth A, Kasper M, et al. Lgr6 marks stem cells in the hair follicle that generate all cell lineages of the skin. *Science*. 2010; 327:1385-1389.
46. Liu W, Shaver TM, Balasa A, et al. Deletion of Porcn in mice leads to multiple developmental defects and models human focal dermal hypoplasia (Goltz syndrome). *Plos One*. 2012; 7(3):e32331.
47. Pemphigus AM. *Dermatology*, 3rd ed. London: Mosby Elsevier; 2012:461-474.
48. Yang CS, Lopez CG, Rana TM. Discovery of nonsteroidal anti-inflammatory drug and anticancer drug enhancing reprogramming and induced pluripotent stem cell generation. *Stem Cells*. 2011; 29:1528-1536.
49. Burchfield JS, Paul AL, Lanka V, et al. Pharmacological priming of adipose-derived stem cells promotes myocardial repair. *J Invest Med*. 2016; 64:50-62.
50. Liu J, Zhu P, Song P, et al. Pretreatment of adipose derived stem cells with curcumin facilitates myocardial recovery via antiapoptosis and angiogenesis. *Stem Cells Int*. 2015; [Epub ahead of print].
51. Kestler HA, Kuhl M. From individual Wnt pathways towards a Wnt signalling network. *Philosophical transactions of the Royal Society of London Series B, J Biol Sci*. 2008; 363:1333-1347.
52. Ueno S, Weidinger G, Osugi T, et al. Biphasic role for Wnt/beta-catenin signaling in cardiac specification in zebrafish and embryonic stem cells. *P Natl Acad Sci USA*. 2007;104:9685-9690.
53. Gros J, Serralbo O, Marcelle C. WNT11 acts as a directional cue to organize the elongation of early muscle fibres. *Nature*. 2009; 457:589-593.
54. Kofron M, Birsoy B, Houston D, et al. Wnt11/beta-catenin signaling in both oocytes and early embryos acts through LRP6-mediated regulation of axin. *Development*. 2007;134:503-513.
55. Zhang X, Yuan X, Shi H, et al. Exosomes in cancer: small particle, big player. *J Hematol Oncol*. 2015; 8(1):83.
56. Luga V, Zhang L, Vitoria-Petit AM, et al. Exosomes mediate stromal mobilization of autocrine Wnt-PCP signaling in breast cancer cell migration. *Cell*. 2012; 151:1542-1556.
57. Gross JC, Chaudhary V, Bartscherer K. Active Wnt proteins are secreted on exosomes. *Nature cell Bio*. 2012; 14:1036-1045.
58. Zhai L, Chaturvedi D, Cumberledge S. Drosophila wnt-1 undergoes a hydrophobic modification and is targeted to lipid rafts, a process that requires porcupine. *J Bio Chem*. 2004; 279:33220-33227.
59. Willert K, Brown JD, Danenberg E, et al. Wnt proteins are lipid-modified and can act as stem cell growth factors. *Nature*. 2003; 423:448-452.
60. Schulte G, Bryja V, Rawal N, et al. Purified Wnt-5a increases differentiation of midbrain dopaminergic cells and dishevelled phosphorylation. *J Neurochem*. 2005;92:1550-1553.
61. Dwyer MA, Joseph JD, Wade HE, et al. WNT11 expression is induced by estrogen-related receptor alpha and beta-catenin and acts in an autocrine manner to increase cancer cell migration. *Cancer Res*. 2010; 70:9298-9308.
62. Guo SC, Tao SC, Yin WJ, et al. Exosomes derived from platelet-rich plasma promote the re-epithelialization of chronic cutaneous wounds via activation of YAP in a diabetic rat model. *Theranostics*. 2017; 7(1): 81-96.